Structural investigation of the Rh(110)-$c(2\times2)$-CN phase

Federica Bondino*
Dipartimento di Fisica, Universitá di Trieste, 34127 Trieste and Laboratorio TASC-INFM, 34012 Trieste, Italy

Alessandro Baraldi†
Sincrotrone Trieste S.C.p.A., S.S. 14 Km 163.5, 34012 Trieste, Italy

Herbert Over
Fritz-Haber-Institut der Max-Planck-Gesellschaft, D-14195 Berlin, Germany

Giovanni Comelli
Dipartimento di Fisica, Universitá di Trieste, 34127 Trieste and Laboratorio TASC-INFM, 34012 Trieste, Italy

Paolo Lacovig, Silvano Lizzit, and Giorgio Paolucci
Sincrotrone Trieste S.C.p.A., S.S. 14 Km 163.5, 34012 Trieste, Italy

Renzo Rosei
Dipartimento di Fisica, Universitá di Trieste, 34127 Trieste and Laboratorio TASC-INFM, 34012 Trieste, Italy
(Received 5 April 2001; published 8 August 2001)

The Rh(110)-$c(2\times2)$-CN phase has been examined by means of scanning tunneling microscopy (STM) and full dynamical low-energy electron diffraction (LEED). From STM large $c(2\times2)$ domains are observed. The detailed LEED-*IV* structural analysis indicates that CN is located in the grooves of the (110) surface, approximately atop second layer rhodium atoms. The CN molecules lie almost flat with their bond axes oriented perpendicular to the rhodium troughs. An outward relaxation of the first substrate interlayer distance and a strong buckling of the second Rh layer are induced by CN adsorption. Calculated and experimental intensity curves are in good agreement. An exhaustive set of other possible adsorption sites and configurations was tested and excluded on the basis of reliability-factor analysis.

DOI: 10.1103/PhysRevB.64.085422 PACS number(s): 68.43.Fg, 61.14.Hg, 68.37.Ef

I. INTRODUCTION

The understanding of CN adsorption properties on Rh is of interest both for large-scale industrial processes, catalysis and fundamental science. The formation of considerable amounts of cyanide intermediates has been reported in many catalytic reactions such as the reduction of NO by ethylene on Rh(111) (Ref. 1) and by propylene on Rh/Al_2O_3.[2] Formation of these cyanide intermediates is an unwanted reaction step in the removal of NO by the three-way catalyst since part of the adsorbed CN hydrogenates and desorbs as poisonous HCN and the remainder decomposes, delaying the desorption of N_2 to higher temperatures. Cyanide species have also been detected during the reaction between NO and carbon on Rh(331) (Ref. 3) and during the interaction of CO and NO on ceria-supported Rh model catalysts (Rh/CeO_x).[4]

Understanding the way CN bonds to the surface is also important in order to provide a detailed description of the microscopic mechanism of industrial processes such as the synthesis of HCN from CH_4, NH_3, and O_2 over Rh-Pt gauzes. CN groups on metal surfaces can also be considered as simple model systems to understand the surface chemistry of organic nitriles.[5] However, an atomistic picture of these reactions cannot be drawn, due to the lack of detailed structural information. To our knowledge, there is only one previous detailed experimental structural study of CN adsorption on a single crystal metal surface [Ni(110)-$c(2\times2)$-CN by photoelectron diffraction.[6]]

From ultraviolet photoelectron spectroscopy (UPS) and penning ionization spectroscopy studies of CN on Pd(111),[7] Pd(110),[8] Ni(110),[9] and Pd(100) (Ref. 10) and CN^- in NaCN (Ref. 11) it was found that CN groups and CN^- have the same order of binding energy levels $4\sigma>1\pi>5\sigma$. Since CN^- and CO are isoelectronic, they were expected to display a similar bonding configuration. However, a wide range of experimental studies of CN adsorption on metal surfaces in ultrahigh vacuum (UHV) environment found that CN does not bind in the typical end-on geometry observed for many other diatomic molecules (e.g., CO, NO, N_2, etc.) both in coordination chemistry and on adsorption.[12] Angle resolved UPS (ARUPS), near edge x-ray absorption spectroscopy and photoelectron diffraction measurements[6–10,13] indeed provided clear evidence that in most of the metal-vacuum interfaces the C-N molecular axis lies essentially parallel to the surface. The explanation of the CN lying-down configuration, unexpected also from coordination chemistry, has been tentatively attributed to prevailing electrostatic and polarization contributions as CN^- bonds to metal surfaces.

The $c(2\times2)$-CN phase on Rh(110) was previously investigated using qualitative LEED, spot profile analysis-LEED (SPA-LEED), x-ray photoemission spectroscopy (XPS), and thermal desorption spectroscopy (TDS).[14] The formation of a sharp $c(2\times2)$ pattern was observed after 1 L of C_2N_2 exposure at 373 K. XPS data showed that at 373 K, complete

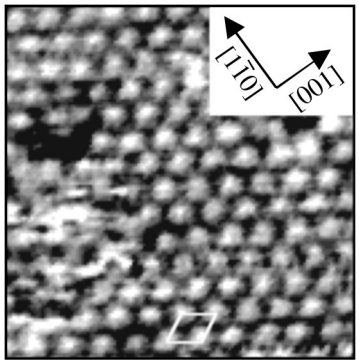

FIG. 1. STM image of $c(2\times2)$-CN on Rh(110) showing the internal structure of this phase. Frame size 70 Å$\times$42 Å, gap Voltage : -0.1 V, tunneling current: 1.0 nA. In this image the drift of the STM scanning stage has been corrected, using software, to make the [001] and [1$\bar{1}$0] directions orthogonal. The overlayer unit cell has been outlined.

dissociation of C_2N_2 into CN groups occurs upon adsorption and this $c(2\times2)$ ordered structure consists of a pure CN overlayer, containing a single CN adsorption state. The full width at half maximum of the (1/2, 1/2) spots, measured by SPA-LEED, indicates that domains of $\approx$200 Å along [1$\bar{1}$0] and $\approx$100 Å along [001] are present on the surface when the $c(2\times2)$ is fully developed. In this paper we report on a detailed structural characterization of this phase by dynamical LEED and STM.

II. EXPERIMENTAL

The LEED-*IV* experiment was carried out in the UHV chamber of the SuperESCA beamline at ELETTRA, equipped with a Fisons rear-view LEED and a 5-degrees-of-freedom manipulator. The LEED-*IV* curves were collected at 180 K and at normal electron beam incidence by using a CCD camera. The STM data were collected at room temperature in a different UHV system by means of a Omicron variable temperature STM. The Rh sample was cleaned by repeated cycles of Ar^+ sputtering and annealing, combined with oxygen and hydrogen treatment. C_2N_2 was produced in situ by thermal decomposition at 570 K of AgCN in a Pyrex tube. The $c(2\times2)$-CN structure was prepared by dosing C_2N_2 at 373 K until a sharp $c(2\times2)$ LEED pattern was observed.

III. RESULTS

A. STM data

STM images of the $c(2\times2)$ structure show a regular and well-ordered pattern with large domains (Fig. 1). A careful analysis of the images reveals that the $c(2\times2)$ structure is present up to the edge of the steps. The size of the domains is consistent with SPA-LEED measurements.[14] In order to determine the registry of the admolecules, line profiles have been measured along [001] and [1$\bar{1}$0] directions. The average distance between the STM bright protrusions along [1$\bar{1}$0] and [001] is twice a Rh(110)-1$\times$1 unit cell. All features have about the same shape and brightness and are arranged in a $c(2\times2)$ structure. However, it is not possible to make a precise attribution of these features to nitrogen, to carbon, to CN groups or to Rh atoms. Therefore we have performed a structural LEED-*IV* analysis in order to obtain an accurate description of the molecular arrangement.

B. LEED-*IV* structural analysis

The quantitative evaluation of LEED-*IV* curves was performed using the full-dynamical LEED program developed by Moritz[15] with an automated search method based on a nonlinear least-squares optimization scheme[16] for the determination of the best fit geometry. The degree of agreement between calculated and experimental intensity data was evaluated using both Pendry (R_P) (Ref. 17) and discrete energies (r_{De}) (Ref. 18) reliability factors. Error bars were estimated from the statistical standard deviation of R_P, calculated according to Pendry.[17] We used up to 9 phase shifts per element. Phase shifts for Rh were the same as those successfully employed in other LEED-*IV* determinations,[19] while for N and C phase shifts were computed from Moruzzi and Li-Tong potentials, respectively.

The real and the imaginary part of the inner potential were first evaluated by a preliminary test calculation of the clean surface LEED-*IV* curves, then fitted during the refinement procedure of the CN-covered surface. The calculation for the clean surface confirmed the presence of a 6.3% contraction of the first ($d_{1,2}=1.26$ Å±0.03 Å) and a 4.1% expansion of the second ($d_{2,3}=1.40$ Å±0.03 Å) Rh interlayer distance, in agreement with previous structural studies.[19,21]

As fractional-order beams are known to be more sensitive to the configuration of superstructure atoms,[20] we used in the LEED analysis an experimental data set dominated by fractional order beams. More specifically, we used all six fractional-order beams and only two of the seven integral-order measured beams (total energy range of 1401 eV) to determine the adsorption geometry of the $c(2\times2)$ phase. After the final optimization the LEED-*IV* curves relative to the remaining five integral order beams have been evaluated too. More than 20 different model structures were explored separately and automatically optimized, starting with structures having one of the two atoms in a high-symmetry site and progressively including the possibility of low-symmetry adsorption sites for both atoms and some relaxation of topmost substrate layers.

Specifically, all possible lying-down structural models with CN oriented along [001] [Fig. 2(a)] or [1$\bar{1}$0] [Fig. 2(b)], adsorbed either on the first or on the second layer Rh atoms were tested. We also considered structural models with CN perpendicularly adsorbed either through C or N in bridge or on-top sites of both the first and the second rhodium layer including also possible bending of the CN molecular axis of static or dynamic nature [Fig. 2(c)]. The latter was simulated using the method of ''split positions'' in the lattice sum mixing approach.[23] The resulting reliability factors are summarized in Table I. The favored adsorption geometry and the associated structure parameters are shown in Fig. 3. The

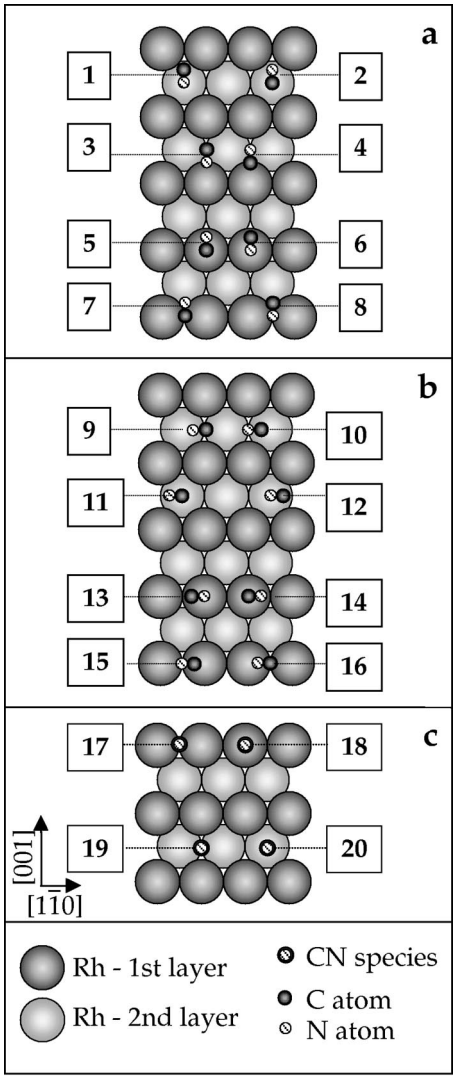

FIG. 2. Adsorption configurations tested in the structural analysis. (a) CN groups lying flat along [001] direction; (b) CN groups lying along [1$\bar{1}$0] direction; (c) CN groups adsorbed perpendicularly to the surface through C or N atom.

comparison between the experimental and the best-fit calculated *IV* curves for all measured integer and fractional beams is shown in Fig. 4.

IV. DISCUSSION

In the best-fit configuration (see Fig. 3) CN adsorbs in a nearly flat geometry in the grooves of the Rh(110) surface, with the CN molecular axis aligned along the [001] direction, tilted by $72.4° \pm 5.9°$ from the surface normal. The molecule is positioned in an asymmetric site, within the grooves of the (110) surface, atop the second layer rhodium atoms. The carbon atom has a threefold coordination, with similar distances from the two nearest neighbor Rh atoms of the top-layer (Rh_I) and the second-layer Rh atom (Rh_{II}) (Rh_I-C distance 1.98 ± 0.10 Å, Rh_{II}-C distance 2.18 ± 0.08 Å). The nitrogen atom is placed in an asymmetric off-atop position. From our analysis we obtain a C-N bond distance of 1.03 ± 0.15 Å. We observe that this value is shorter than the expected C-N distance, but it should be also noted that, in our determination, the precision of this parameter is particulary poor. The large error bar is mainly due to the uncertainty in the determination of the atomic coordinates parallel to the surface. For reference, the length of a formal C-N triple bond is 1.16 Å,[24] corresponding to the C-N bond length in the C_2N_2 free molecule. The C-N bond length obtained from total energy calculations on Pt_{25} clusters[25] and on Ni_{28} clusters[26] is 1.18–1.19 Å, while the value found for CN on Ni(110) (Ref. 6) was 1.25 ± 0.12 Å. CN adsorbed species lead to a mean expansion of the first substrate layer, if compared to the bulk interlayer distance, as frequently reported for adsorption of electronegative species.[12] The outward relaxation induced by CN is even larger when compared to the clean rhodium surface which presents a contraction of the first layer distance. CN has also a particularly strong local effect: the molecule induces a significant periodic buckling of the second Rh layer, by pushing the Rh atom of the second layer on which it sits by 0.09 ± 0.02 Å relative to the Rh

TABLE I. Best-fit reliability factors of models displayed in Fig. 2. The values without brackets are the best-fit *R* factors obtained keeping at least one of the two atoms fixed at a high symmetry site (top or bridge). The values within the brackets are the best *R* factors obtained by relaxing the position of both atoms in the lying-down models (1–16), but keeping C-N molecular axis either along [001] or [1$\bar{1}$0]. Models 17–20 are configurations with CN bonded perpendicular to the surface either through C (Rh-C-N) or N (Rh-N-C) and the values in the brackets are obtained by allowing a tilt of the C-N axis.

Model (see Fig. 2)	R_P	r_{De}
1	0.35 (0.26)	0.30 (0.26)
2	0.39 (0.29)	0.47 (0.33)
3	0.62 (0.61)	0.51 (0.49)
4	0.61 (0.60)	0.51 (0.52)
5	0.56 (0.58)	0.61 (0.51)
6	0.56 (0.55)	0.52 (0.52)
7	0.43 (0.42)	0.39 (0.37)
8	0.37 (0.37)	0.39 (0.39)
9	0.40 (0.40)	0.48 (0.48)
10	0.41 (0.38)	0.46 (0.38)
11	0.40 (0.38)	0.48 (0.47)
12	0.42 (0.41)	0.48 (0.48)
13	0.66 (0.61)	0.63 (0.58)
14	0.64 (0.64)	0.59 (0.59)
15	0.63 (0.61)	0.58 (0.58)
16	0.65 (0.65)	0.55 (0.55)
17 (Rh-N-C)	0.67 (0.61)	0.46 (0.52)
18 (Rh-N-C)	0.62 (0.62)	0.63 (0.63)
19 (Rh-N-C)	0.63 (0.62)	0.45 (0.45)
20 (Rh-N-C)	0.50 (0.36)	0.48 (0.38)
17 (Rh-C-N)	0.66 (0.60)	0.48 (0.53)
18 (Rh-C-N)	0.63 (0.69)	0.62 (0.59)
19 (Rh-C-N)	0.64 (0.64)	0.47 (0.46)
20 (Rh-C-N)	0.48 (0.37)	0.51 (0.41)

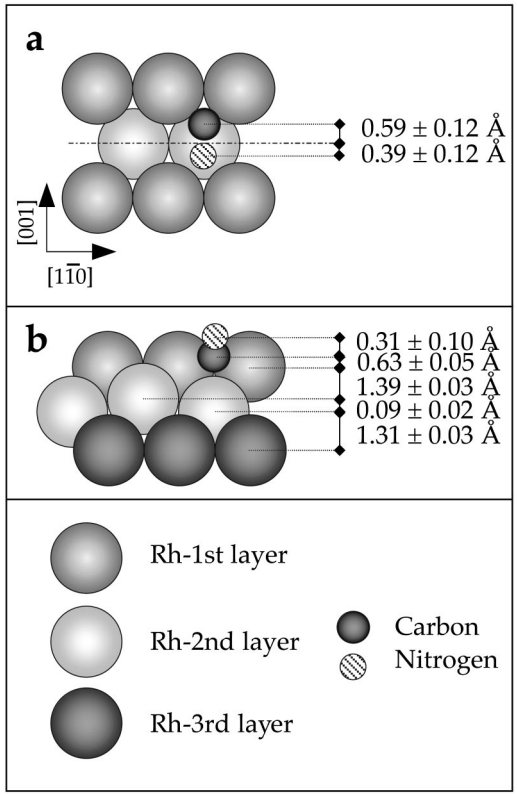

FIG. 3. Best-fit surface arrangement for the Rh(110)-$c(2\times2)$-CN phase with associated structure parameters and error bars; (a) top view; (b) side view.

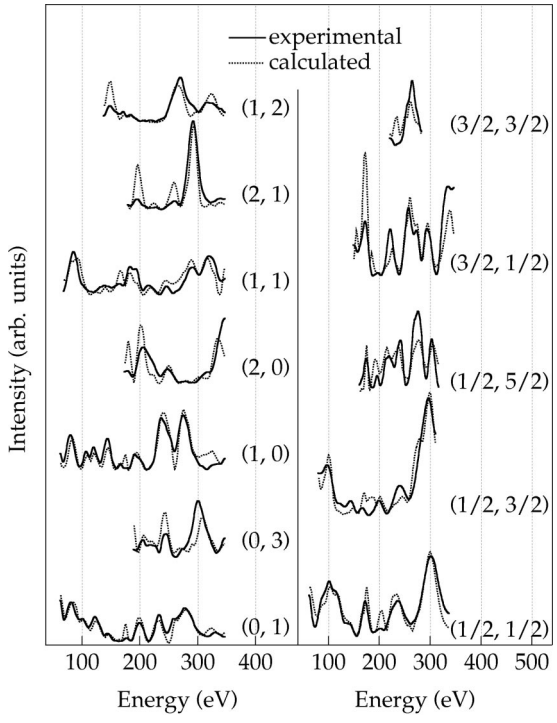

FIG. 4. Experimental (full line) and calculated (dotted line) *IV* curves for the optimum structure depicted in Fig. 2 ($R_P=0.26, r_{De}=0.26$).

atoms of the same layer which are not covered by CN. This periodic rumpling of the second Rh layer could explain the observed particularly intense fractional order beams of the $c(2\times2)$ LEED pattern. Both CN-induced global (outward relaxation of the top layer) and local (buckling of the second layer) changes in the substrate contribute to increase the distance between the first and the second Rh layer.

The best-fit adsorption configuration yielded $R_P=r_{De}=0.26$, which are quite low for a molecular adsorption system and therefore support the proposed geometry. In particular, all configurations with CN adsorbed on the first Rh layer, with C-N molecular axis perpendicular to the surface or along [1$\bar{1}$0] can be safely excluded because they always give a R_P higher than 0.60, diverging significantly from the best-fit adsorption structure. A better agreement is generally achieved for CN sitting approximately atop a second layer Rh atom with C-N molecular axis either perpendicular to the surface or along [1$\bar{1}$0]. Also these two models can be ruled out, though in their best-fit Pendry reliability factors were 0.36 and 0.38, respectively, because these values are outside our estimated standard deviation of R_P (0.04); furthermore optimized metal-carbon and metal-nitrogen distances were too short for these configurations, compared to typical values reported in literature. Another low value of the *R* factor is achieved for CN on the first Rh layer, with N located at a bridge site with C-N molecular axis oriented along [001] direction. But also this geometry can be excluded because the associated *R* factor (0.37), which does not improve for nitrogen low-symmetry site position, is out of the limits of our estimated confidence interval.

This full dynamical LEED study confirms that CN on Rh(110) follows the general adsorption behavior of CN species, preferentially bonded with C-N axis nearly parallel to the surface in metal-vacuum interfaces. In particular, the local adsorption geometry of CN on Rh(110) agrees nicely with that of the $c(2\times2)$-CN on Ni(110) determined by photoelectron diffraction.[6] In the latter case the molecule was found to be located within the Ni(110) grooves, on top a second layer Ni atom, oriented along the [001] direction, with nitrogen atom bridging two first layer Ni atoms and carbon bonded both to the first and second layer Ni atoms.

Interesting similarities, probably correlated to the almost identical adsorption configuration between $c(2\times2)$-CN adlayers on Ni(110) and Rh(110), are also observed in the thermal evolution of these structures. From both $c(2\times2)$-CN adlayers no C_2N_2 desorption has been detected. On both surfaces CN decomposes via C-N bond scission at $\approx$500–550 K, with nitrogen desorbing at 800 K, leaving carbon on the surface.[27] Differently, on Pd(110) no CN dissociation occurs but, when the surface is heated, C_2N_2 desorbs with the recombination of CN groups on the surface.[22,28] Previous polarization dependent ARUPS studies[8] have indicated that in the Pd(110)-$c(2\times2)$-CN phase the CN species are also flat-lying in-groove species, but oriented along the [1$\bar{1}$0] direction. This different thermal behavior can be due to the lower reactivity of Pd towards CN dissociation, but it can also be linked to the different starting CN adsorption geometry. Alignment of the

adsorbed CN molecules in the $[1\bar{1}0]$ direction can influence their thermal evolution both by determining a lower barrier for surface diffusion and by favoring the formation of the linear C_2N_2 molecule when two CN fragments meet in the head-to-head configuration. When oriented along the $[1\bar{1}0]$ direction, into the grooves of the (110) surface, CN species can diffuse more easily and thus recombine and leave the surface as C_2N_2. In the case of Ni(110) and Rh(110) the diffusion is hindered and the energy barrier for diffusion is likely to be higher than the energy barrier for C-N bond scission, so that decomposition occurs prior to CN recombination.

V. CONCLUSIONS

By means of LEED-*IV* calculations and STM images we have determined the detailed atomic-scale structure of the $c(2\times2)$-CN phase on Rh(110), formed by the dissociative adsorption of C_2N_2 at 373 K. An exhaustive set of different models was explored and automatically optimized by the LEED-*IV* structural analysis. The result indicates that the CN adsorption configuration on Rh(110) is almost identical to that of the $c(2\times2)$-CN on Ni(110). In the best-fit configuration CN molecules lie almost flat and are located in the grooves of the (110) surface, perpendicular to the rhodium troughs, approximately atop second layer atoms. CN adsorption induces an outward relaxation of the first substrate interlayer distance and a strong buckling of the second Rh layer.

ACKNOWLEDGMENTS

F.B. thanks Dr. Y. D. Kim and C. Africh for their help, F. P. Netzer for a critical reading of the manuscript and also gratefully acknowledges the warm hospitality of the members at the Institut für Physikalische Chemie of the Fritz-Haber-Insitut in Berlin during her stay. This work has been supported by the Italian INFM, by MURST under the program ''COFIN99'' and by Sincrotrone Trieste S.C.p.A.

*Corresponding author. E-mail: federica.bondino@elettra.trieste.it
†Present address: Dipartimento di Fisica, Universitá di Trieste, 34127 Trieste and Laboratorio TASC-INFM, 34012 Trieste, Italy

[1] R.M. van Hardeveld, A.J.G.W. Schmidt, R.A. van Santen, and J.W. Niemantsverdriet, J. Vac. Sci. Technol. A **15**, 1642 (1997).
[2] G.R. Bamwenda, A. Obuchi, A. Ogata, and K. Mizuno, Chem. Lett. **11**, 2109 (1994).
[3] L.A. DeLouise and N. Winograd, Surf. Sci. **154**, 79 (1985).
[4] D.R. Mullins, L. Kundakovic, and S.H. Overbury, J. Catal. **195**, 169 (2000).
[5] F.P. Netzer and M.G. Ramsey, Crit. Rev. Solid State Mater. Sci. **17**, 397 (1992).
[6] N.A. Booth, R. Davis, D.P. Woodruff, D. Chrysostomou, T. McCabe, D.R. Lloyd, O. Schaff, V. Fernandez, S. Bao, K.-M. Schindler, R. Lindsay, J.T. Hoeft, R. Terborg, P. Baumgärtel, and A.M. Bradshaw, Surf. Sci. **416**, 448 (1998).
[7] M.E. Kordesch, W. Stenzel, and H. Conrad, Surf. Sci. **186**, 601 (1987).
[8] M.G. Ramsey, G. Rosina, F.P. Netzer, H.B. Saalfeld, and D.R. Lloyd, Surf. Sci. **218**, 317 (1989).
[9] M.G. Ramsey, D. Steinmüller, F.P. Netzer, S. Köstlmeier, J. Lauber, and N. Rösh, Surf. Sci. **307-309**, 82 (1994).
[10] K. Besenthal, G. Chiarello, M.E. Kordesch, and H. Conrad, Surf. Sci. **178**, 667 (1986).
[11] H. Pulm, B. Marquardt, H.-J. Freund, R. Engelhardt, K. Seki, U. Karlsson, E.E. Koch, and W. von Niessen, Chem. Phys. **92**, 457 (1985).
[12] H. Over, Prog. Surf. Sci. **58**, 249 (1998).
[13] J. Somers, M.E. Kordesch, Th. Lindner, H. Conrad, and A.M. Bradshaw, Surf. Sci. **188**, L693 (1987).
[14] F. Bondino, A. Baraldi, G. Comelli, and F.P. Netzer, Surf. Sci. **461**, 31 (2000).
[15] W. Moritz, J. Phys. C **17**, 353 (1984).
[16] G. Kleinle, W. Moritz, and G. Ertl, Surf. Sci. **238**, 119 (1990); H. Over, U. Ketterl, W. Moritz, and G. Ertl, Phys. Rev. B **46**, 15 438 (1992).
[17] J.B. Pendry, J. Phys. C **13**, 937 (1980).
[18] G. Kleinle, W. Moritz, D.L. Adams, and G. Ertl, Surf. Sci. **219**, L637 (1989).
[19] M. Gierer, H. Over, G. Ertl, H. Wohlgemuth, E. Schwarz, and K. Christmann, Surf. Sci. **297**, L73 (1993).
[20] H. Over, M. Gierer, H. Bludau, G. Ertl, and S.Y. Tong, Surf. Sci. **314**, 243 (1994).
[21] W. Nichtl, N. Bickel, L. Hammer, K. Heinz, and K. Müller, Surf. Sci. **188**, L729 (1987).
[22] M.G. Ramsey, G. Rosina, F.P. Netzer, H.B. Saalfeld, and D.R. Lloyd, Surf. Sci. **217**, 140 (1989).
[23] H. Over, W. Moritz, and G. Ertl, Phys. Rev. Lett. **70**, 315 (1993).
[24] J. E. Huheey, E. A. Keiter, and R. L. Keiter, *Inorganic Chemistry: Principles of Structure and Reactivity* (Harper Collins College Publishers, New York, 1993), Sec. A-30.
[25] W. Daum, F. Dederichs, and J.E. Müller, Phys. Rev. Lett. **80**, 766 (1998).
[26] H. Yang, T.C. Caves, and J.L. Whitten, J. Chem. Phys. **103**, 8756 (1995).
[27] M.G. Ramsey, D. Steinmüller, F.P. Netzer, M. Neuber, L. Ackermann, J. Lauber, and N. Rösch, Surf. Sci. **260**, 163 (1992).
[28] A. Baraldi, S. Lizzit, M.G. Ramsey, and F.P. Netzer, Surf. Sci. **416**, 214 (1998).